

# Scale-free structure of brain functional networks

Victor M. Eguíluz,<sup>1</sup> Guillermo Cecchi,<sup>2</sup> Dante R. Chialvo,<sup>1,3</sup> Marwan Baliki,<sup>3</sup> and A. Vania Apkarian<sup>3</sup>

<sup>1</sup>*Instituto Mediterráneo de Estudios Avanzados, IMEDEA (CSIC-UIB), E07122 Palma de Mallorca, Spain*

<sup>2</sup>*IBM T.J. Watson Research Center, 1101 Kitchawan Rd., Yorktown Heights, NY 10598, USA.*

<sup>3</sup>*Department of Physiology, Northwestern University, Chicago, Illinois, 60611, USA.*

(Dated: February 9, 2019)

The dynamic interaction of brain regions, during behavior or even at rest, creates and continuously reconfigures complex networks of correlated dynamics. Using functional magnetic resonance imaging we studied the topological properties of these networks defined by the links between the highest correlated voxels. We report here that the degree distribution and the probability of finding a link vs. distance both decay as a power law. Furthermore the path length between any two sites is a relatively small value around 10. The clustering coefficient we find is several orders of magnitude larger than in the case of the equivalent random network and much larger than that of a null model with random rewiring. All these features are signatures of scale-free networks with small-world properties.

PACS numbers:

An ultimate goal of neuroscience is to be able to read human thoughts, *i.e.* to decipher brain spatio-temporal patterns of neural activity. The richness of human behavior is reflected in the dynamical patterns of brain activity on a network of gargantuan size and complexity[1]. This letter describes the characteristic features of these brain networks, as seen using functional magnetic resonance imaging (fMRI)[2, 3, 4], and discuss their generality in the context of recent understanding of complex networks (for reviews see [5, 6, 7, 8]).

It is widely recognized, but not so often expressed in useful quantifiable terms, that relevant brain activity in a given area can be correlated with far away and apparently unrelated regions. In qualitative terms this means that, for instance, a concurrent sound or simply imagery can influence thoughts or pain perception. In fact, using functional magnetic resonance imaging one can see and measure the extent of these correlations. Figure 1 shows that neural activity between any two areas of the brain exhibits correlations of long range. The plot is an example of the average correlation function of human brain activity recorded with functional magnetic resonance [9]. In this case, the subject is cyclically moving his fingers, but similar results can be obtained under other behaviors. It is clear that there is a slow decay of the correlation function  $r$  with distance  $\Delta$ . From the shortest scale analyzed (the voxel's length) to the system size (the brain "radius") there is no typical length for the correlations, instead activity is correlated at all scales as  $r(\Delta) \sim \Delta^{-\beta}$ , a fact that often is indicative of an underlying scale-free structure.

How to dissect the underlying network suggested by Fig. 1? A fruitful approach to study systems composed by large number of non-linear interacting elements is network analysis, *i.e.* the study of connectivity and dynamic properties of the networks spanned by those elements [5, 6, 7, 8]. Although it is undeniable that such inter-

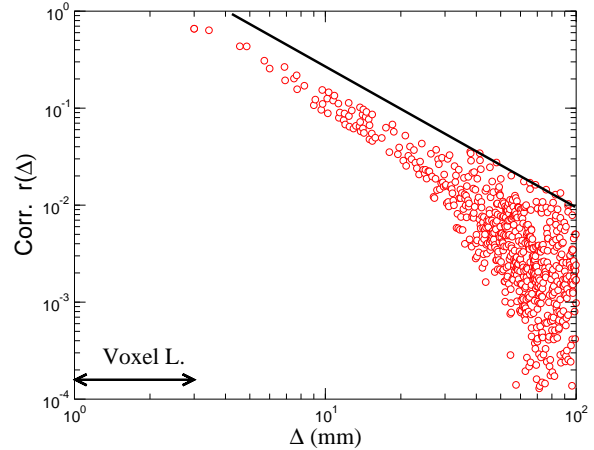


FIG. 1: Average spatial two-points correlation function of brain activity recorded using functional magnetic resonance imaging (Subject SL). The graph is the average taken from 400 consecutive measures of the 147456 brain sites ( $64 \times 64 \times 36$  voxels) of size  $3.475 \times 3.475 \times 3$  mm $^3$ . The arrow indicates the smallest length scale analyzed (*i.e.* voxel's length), and the line a decay  $r(\Delta) \sim \Delta^{-\beta}$  with  $\beta=3/2$ .

acting elements are a realistic assumption for the brain, less obvious is how the brain activity exposed by fMRI need to be unveiled to visualize the underlying network. In this letter we choose, for simplicity, to define as "connected" those voxels whose temporal evolution is correlated beyond some pre-established value, an approach already used by Dodel et al.[10]. In other words, pairs of voxels whose correlation  $r$  exceeds a certain threshold  $r_c$  will be considered functionally linked, and therefore participating in the global network of intercommunicated units that is the substrate of a behavioral state. Further numerical analysis is performed on the resulting networks in order to characterize their properties.

In these experiments each snapshot of the brain activ-

ity revealed by fMRI comprises  $64 \times 64 \times 36$  voxels of size  $3.475 \times 3.475 \times 3$  mm<sup>3</sup>. The activity of each voxel is recorded every 2.5 seconds obtaining 400 time steps for each task. The activity of voxel  $x$  at time  $t$  is called  $V(x, t)$ . We calculate the linear correlation coefficient between any pair  $x_1$  and  $x_2$  of voxels as

$$r(x_1, x_2) = \frac{\langle V(x_1, t)V(x_2, t) \rangle - \langle V(x_1, t) \rangle \langle V(x_2, t) \rangle}{\sigma(V(x_1))\sigma(V(x_2))}, \quad (1)$$

where  $\sigma^2(V(x)) = \langle V(x, t)^2 \rangle - \langle V(x, t) \rangle^2$ , and  $\langle \cdot \rangle$  represent temporal averages.

In order to obtain a network we consider that two voxels have a link if their correlation coefficient is larger than a given threshold  $r_c$ . If  $r_c$  is too low, we will find that most of the voxels are connected to each other, while if the threshold is too high the voxels are mostly isolated from the rest.

In Fig. 2a, we plot the degree distribution for one subject in a finger tapping task. Degree is the mathematical term for connectivity, being here the number of links a voxel has. We find that the degree distribution has a skewed distribution with a tail approaching a power law distribution with an exponent around 2. As the threshold  $r_c$  is decreased a maximum appears which shifts to the right as  $r_c$  is lowered.

In Fig. 2b we have plotted the degree distribution for another subject performing on-off finger tapping with three different protocols. In each case the subject is moving his fingers, in one case is instructed verbally to start and stop tapping, in the other one the clue is a small green/red dot in a video screen and in the last one the clue is the entire screen turning green or red. Despite the behavioral differences in the task, we find similar power law decay with the same exponents as in the subject results plotted in Fig. 1a. We have compared our results for the degree distribution with a randomization of the data. We randomly shuffled the original time sequence of each voxels signal, keeping other statistical properties for each voxel the same. As expected, the degree distribution is now a Gaussian distribution (see Fig. 2c) where the mean and the width depends on  $r_c$ . Note the different values of the threshold we need to use in the random case  $r_c \simeq 0.1$  in comparison the original data  $r_c \simeq 0.7$ .

We have performed an average over 7 subjects and 22 tasks (3 tasks in 6 subjects and 4 tasks for 1 subject). The average of the degree distribution is shown in Fig. 2d. The tail decays as a power law, for  $r_c = 0.6$  the exponent is 2, for  $r_c = 0.7$  is 2.1 and for  $r_c = 0.8$  is 2.2. From a biologist view the power law is telling a simple but significant fact: it exists the possibility of at least few brain sites which will have "access" to the entire brain, those few nodes are, at the same time, comparatively many more than in a randomly connected network.

Other quantities describing the statistical properties of networks include the path length and the clustering.

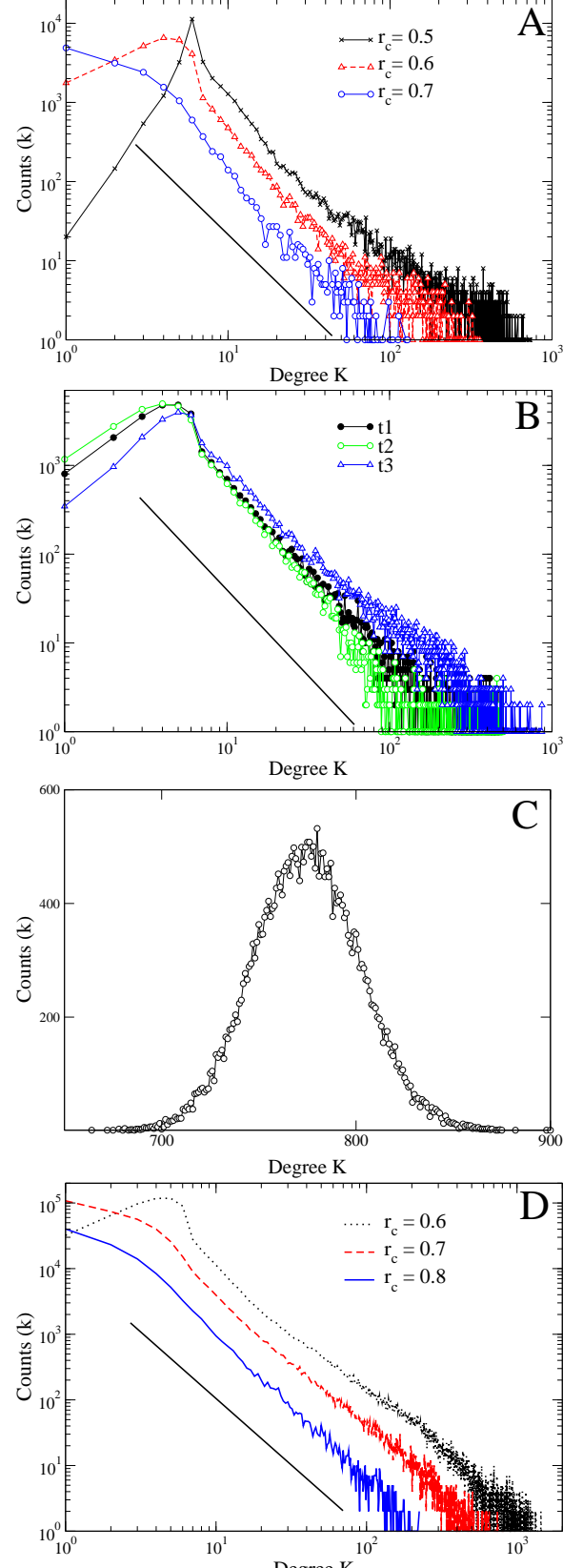


FIG. 2: Brain degree distribution: (A): Data obtained during a finger tapping task. Different symbols represent results for the thresholds  $r_c=0.5$ , 0.6 and 0.7. (subject SL). (B): Data from a different subject than (A) obtained during three different tasks (subject CW, threshold  $r_c=0.6$ ) (C) A random rearrangement of the raw data plotted in (A) showing no scaling. (D) Average from seven subjects showing scale-free degree distribution. Straight lines illustrate a decay of  $k^{-2}$ .

We define each one before examining our results. The *path length* between two voxels is the minimum number of links necessary to connect both voxels. *Clustering* is the fraction of connexions between the topological neighbors of a voxel with respect to the maximum possible. If voxel  $i$  has degree  $k_i$ , then the maximum number of links between the  $k_i$  neighbors is  $k_i(k_i - 1)/2$ . If  $E_i$  is the number of links connecting the neighbors then the clustering of voxel  $i$ ,  $C_i = 2E_i/k_i(k_i - 1)$ . The average clustering of a network is given by  $C = 1/N \sum_i C_i$ , where  $N$  is the number of voxels. *Density*  $\rho$  is the ratio between the number of links and the total number of links (*i.e.*  $N(N - 1)/2$ ) in a fully connected network. *Clustering vs degree*: The average clustering over voxels with the same degree  $C(k) = 1/N_k \sum_{j=\{i|k_i=k\}} C_j$ , where the sum runs over the  $N_k$  voxels with degree  $k$ .

In Table 1 we show a summary of the topological properties of the networks analyzed. The table shows the averages values ( $n = 22$  tasks) obtained for each threshold ( $r_c$ , first column) used to define the networks. Listed are the number of nodes  $N$ , the clustering coefficient  $C$ , the shortest path length  $L$ , the average degree  $\langle k \rangle$ , the density  $\rho$  and the decay of the degree distribution  $\lambda$ . Note that as the threshold increases the method selects more correlated networks. As expected in this case the number of nodes with at least one link decreases as well as the average degree and the path length. However, the clustering coefficient and the density remain basically the same and in all cases the former is four orders of magnitude larger than the latter (which corresponds to the clustering of a random network). This, together with the relatively short path length, are the signature of a small-world structure [11]. Note that the property is robust because it does not depend on the numerical parameters  $r_c$  used to unveil the network.

An informative test is to recalculate these coefficients for the null model introduced by Maslov and Sneppen [15]. In this case the original network is randomly rewired, with nodes having similar degrees being permuted, say for instance the link connecting node(i,j) is permuted with the one connecting node(k,l). In this way the degree distribution is maintained while all other correlations (including clustering) are destroyed. In our case, we found that after rewiring the computed value for the average clustering  $C$  drops to 0.02 and the shortest path length  $L$  to 4.

$r_c$	$N$	$C$	$L$	$\langle k \rangle$	$\rho$	$\lambda$
0.6	31503.2	0.144	11.42	13.41	0.000428	2.0
0.7	17174.6	0.127	12.95	6.29	0.000369	2.1
0.8	4891.3	0.156	5.96	4.12	0.000893	2.2

Table 1: Statistical properties of fMRI human brain functional networks.

Network	$N$	$C$	$L$	$\langle k \rangle$	$\rho$
C. Elegans	282	0.28	2.65	14	0.025
Macaque VC	32	0.55	1.77	9.85	0.318
Cat Cortex	65	0.54	1.87	17.48	0.273

Table 2: Previously reported networks statistics. C. Elegans [11], Macaque Visual Cortex and Cat Cortex [1]

To the best of our knowledge, there are only two previous reports on these statistics in brain-like networks. The first study analyzes the relatively small networks of the C. Elegans [11]. The other work [1, 12] reports on the properties of two neuro-anatomical databases, the macaque visual cortex [13] and the cat cortex [14]. The main quantitative conclusions of these reports, condensed in Table 2, can be contrasted with the present results. First of all, our method allows us to build and analyze networks of size orders of magnitude larger. In that sense this paper describes the largest biological network in the literature. With this caveats in mind, comparison with the previous two reports indicate the following: the clustering in our case is smaller in absolute value, but still is orders of magnitude larger than the random case ( $10^{-1}$  vs  $10^{-4}$ ), while in the previous reports the clustering of the random case is one order of magnitude lower in the best case. Interestingly the average connectivity  $\langle k \rangle$  in all cases is of the same order, despite the huge differences in networks' origins and sizes. One is tempted to speculate that it could be reflecting some network construction constraints. Overall these quantitative features suggest that the human brain network analyzed here has small world properties, a fact that was speculated earlier on [11].

We have also analyzed the dependence of the clustering of a voxel with respect to its degree. It has been found that many networks show what has been called a hierarchical organization  $C(k) \sim k^{-\alpha}$  [16, 17]. However we don't find this signature for the networks we have analyzed. It could be that the voxel volume (few  $\text{mm}^3$ ) is too large to inspect the lower end of the hierarchy. The results are similar to the behavior observed in other networks subjected to spatial constraints, such as the internet at the router level and the power grid [17]. Thus the absence of hierarchical organization could also be due to the fact that the brain is constrained to develop in a 3D volume. Another feature we found lacking scaling is the average degree of a neighbor  $\langle k_1 \rangle$  versus the node degree  $\langle k_0 \rangle$ . All these issues deserve further analysis.

Finally we have computed the probability of finding a link as a function of the distance from a node. This is plotted in Fig. 3 where it is apparent a power decay of the probability with an exponent of 2.3. Although “physical” distance needs to be considered with caution, because of the abundant cortical folding, this feature is nevertheless consistent with the idea of the functioning brain as a scale-free structure.

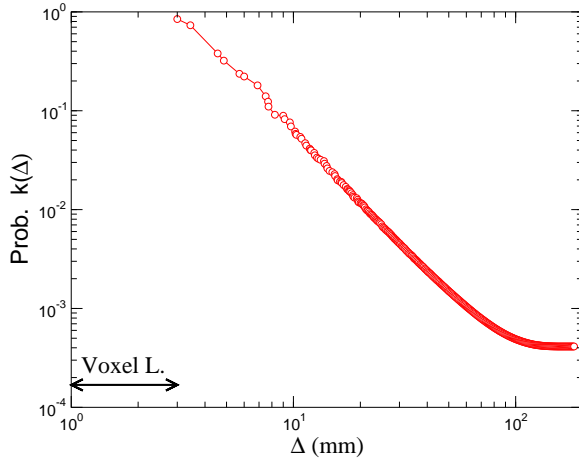


FIG. 3: Probability of finding a link between two nodes separated by a distance  $x < \Delta$ . Averages from  $n = 22$ , same data set as in Fig. 2d using  $r_c = 0.6$ .

In summary, this letter shows aspects of human brain activity that can be described as a scale-free network, a robust finding across subjects and parameters. While the idea have been discussed previously several times, the present report is the first quantitative evidence at large scale supporting such view. . Discussing the implication for brain functioning can be tempting, since a network with such properties shows resistance to failure, facility of synchronization, and fast signal processing [5]. It will be desirable on one hand to provide a theoretical framework for the scaling laws uncovered here and on the other hand to verify these scaling properties using other imaging technologies such as magnetic electroencephalography. Finally, a challenge is to design fruitful experimental paradigms to investigate the biological relevance of the network properties in health and disease.

We acknowledge financial support from MCyT (Spain) under project BFM2002-04474-C02-01 and NIH NINDS (USA) under grants 42660 and 35115. DRC is grateful for the hospitality and support of the Universitat de les Illes Balears, Palma de Mallorca, Spain.

bral Cortex **10**, 127-141 (2000).

- [2] B. Biswal, F.Z. Yetkin, V.M. Haughton, J.S. Hyde. *Functional connectivity in the motor cortex of resting human brain using echo-planar MRI*. Magnet. Reson. Med. **34**, 537-541 (1995).
- [3] M.J. Lowe, M. Dzemidzic, J.T. Lurito, V.P. Mathews, M.D. Phillips. *Correlations in low-frequency BOLD fluctuations reflect cortico-cortical connections*. Neuroimage, **12**, 582-587 (2000).
- [4] D. Cordes, V. Haughton, J.D. Carew, K. Arfanakis, K. Maravilla, *Hierarchical clustering to measure connectivity in fMRI resting-state data*. Magnetic Resonance Imaging **20**, 305-317 (2002).
- [5] S.H. Strogatz, *Exploring complex networks*. Nature **410**, 268-276 (2001).
- [6] R. Albert, A.-L. Barabási, *Statistical mechanics of complex networks*. Rev. Mod. Phys. **74**, 47 (2002).
- [7] S. N. Dorogovtsev, J. F. F. Mendes, *Evolution of networks*. Adv. Phys. **51**, 1079 (2002).
- [8] M.E.J. Newman, *The structure and function of complex networks*. SIAM Review **45**, 167-256 (2003).
- [9] The subject is doing a finger tapping task opposing fingers 1 and 2 during 10 seconds, and then resting during 10 sec. Similar decays are observed, though, during other tasks, including resting conditions. Since correlations can be generated by the fMRI' hardware and software controls were examined to reject this possibility. They include the examination of similar correlations and network analysis on a water filled bottle as a phantom brain, rejection of data sets with head motion and filtering to suppress the cardiorespiratory influences as discussed in [4].
- [10] S. Dodel, J.M. Herrmann, T. Geisel, *Functional connectivity by cross-correlation clustering*. Neurocomputing **44**, 1065-1070 (2002).
- [11] D.J. Watts, S.H. Strogatz, *Collective dynamics of small-world networks*. Nature **393**, 440-442 (1998).
- [12] O. Sporns, G. Tononi, *Classes of network connectivity and dynamics*. Complexity **7**, 28-38 (2003).
- [13] D.J. Felleman, D.C. Van Essen, *Distributed hierarchical processing in the primate cerebral cortex*. Cerebral Cortex **1**, 1-47 (1991).
- [14] J.W. Scannell, G.A.P.C. Burns, C.C. Hilgetag, M.A. O'Neil, M.P. Young, *The connectional organization of the cortico-thalamic system of the cat*. Cerebral Cortex **9**, 277 (1999).
- [15] S. Maslov, K. Sneppen, *Specificity and stability in topology of protein networks*. Science **296**, 910-913 (2002).
- [16] E. Ravasz, A.L. Somera, D.A. Mongru, Z.N. Oltvai, A.-L. Barabási, *Hierarchical organization of modularity in metabolic networks*. Science **297**, 1551-1555 (2002).
- [17] E. Ravasz, A.-L. Barabási, *Hierarchical Organization in Complex Networks*. Phys. Rev. E **67**, 026112 (2003).